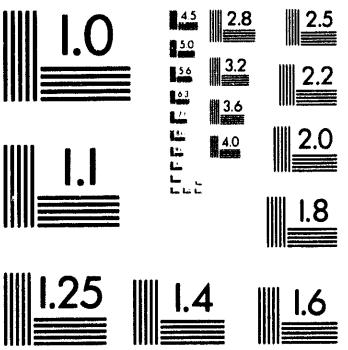
1.0
1.1
1.25
1.4
1.6
1.8
2.0
2.2
2.5
2.8
3.2
3.6
4.0
4.5
5.0
5.6
6.3

1 of 1

Submitted to: Vibrations at Surfaces VII
Santa Margherita, Italy June 13-17, 1993

BNL-49557
Conf-9306281--1

Dipole Forbidden Vibrational Modes for NO and CO on Cu Observed in the Far IR

C.J. Hirschmugl[a,b], P. Dumas[c], Y.J. Chabal[d], F.M. Hoffmann[e], M. Suhren[c] and G.P. Williams[a].

[a] National Synchrotron Light Source, Brookhaven National Lab, Upton, NY 11973, USA.

[b] Department of Applied Physics, Yale University, New Haven CT 06520, USA.

[c] LURE, Centre Universitaire Paris-Sud, F-91405 Orsay, France.

[d] AT&T Bell Labs, 600 Mountain Avenue, Murray Hill, NJ 07974, USA.

[e] EXXON Research & Engineering, Corporate Research Laboratories, Annandale, NJ 08801, USA.

IRRAS spectra of NO/Cu(111) and ($\sqrt{3}\times\sqrt{3}$)R30° coverage of CO/Cu(111) in the range 3000-180 cm^{-1} show both the adsorbate internal modes and features assigned to the hindered rotational modes. These dipole-forbidden features are characterized by asymmetric (mostly negative) absorption lineshapes and are accompanied by a change in broadband absorption. The shape and intensity of this broadband absorption is well accounted for by a scattering model.

1. INTRODUCTION

A breakdown of the dipole selection rule for adsorbate vibrational modes on metal surfaces has been observed for H/W(100) [1] and CO on Cu surfaces [2,3]. The observed features are dipole forbidden because they involve vibrations parallel to the metallic surfaces. They typically have asymmetric lineshapes and are accompanied by an electronic broadband absorption. These observations are consistent with the non-adiabatic coupling of the vibrations with electronic transitions polarized parallel to the surface [4].

The nature of the broadband absorption is important in understanding the mechanism of the infrared activity. The broadband absorption associated with the H/W(100) system [1], for instance, displays a strong peak characteristic of a sharp surface electronic state. Non-adiabatic coupling of the W-2H asymmetric stretch or wag modes to such a state is therefore likely. In contrast, the broadband absorption of the CO/Cu system [2,3] increases asymptotically beyond 2000 cm^{-1}. The lack of a clear surface state absorption has encouraged a different theoretical model, based on the scattering of substrate free electrons at the surface and the interaction of the adsorbate parallel vibrations (e.g. hindered rotation) to these electron [5]. In this model, the parallel vibrational modes appear as anti-absorption features in the absorption spectra. One of the predictions of this model is the universality of the phenomenon, regardless of the specific induced surface states.

In this paper, we therefore extend our work to the NO/Cu system. NO has a different bonding configuration from CO: more highly coordinated than on-top, as inferred from EELS data [6]. It may also have a tilted configuration, as suggested by recent ab-initio cluster calculations [7] and two photon photoemission [8]. The electronic structure of the CO/Cu and NO/Cu surfaces is therefore quite different, but the character of the normal modes and conduction electrons quite similar. A comparison of the vibrational and broadband absorption of CO/Cu and NO/Cu systems is therefore a partic-

*Work performed under the auspices of the U.S. Department of Energy, under contract DE-AC02-76CH00016.

ularly good check of the various theories.

We have used far infrared synchrotron radiation to investigate the low frequency modes (< 500 cm^{-1}) on these two surfaces. These modes are almost 2 orders of magnitude weaker than typical intramolecular modes, thus providing a considerable instrumental challenge. We find that the dipole forbidden hindered rotation which was observed for CO is also seen for the NO/Cu system while the dipole allowed Cu-NO stretch is too weak to be observed. The broadband absorption is characterized by a slow asymptotic behavior similar to that of the CO/Cu system. These observations are in qualitative agreement with the scattering model.

2. EXPERIMENTAL PROCEDURES

The experiments were performed at the National Synchrotron Light Source using beamline U4-IR, which is described elsewhere [9-12]. The white beam is focused through a wedged CsI window, then collimated into a Nicolet 20F Michelson interferometer. This vacuum instrument is equipped with a silicon beamsplitter optimized for the 700 to 30 cm^{-1} but usable up to 2500 cm^{-1} without changing the optical setup. The lower frequency for the present experiments is limited to 180 cm^{-1} by the CsI windows on the beamline and the UHV chamber. The beam emerging from the interferometer is focussed (f10) into a UHV chamber and reflected at grazing incidence (~88°) off a single crystal of dimensions 25 mm x 6mm x 3 mm. Finally, the beam is refocused onto a boron doped silicon bolometer at 4.2 K for low frequency measurements (500 - 180 cm^{-1}) or a copper-doped germanium photoconductive detector at 4.2 K for high frequency measurements (2500 - 300 cm^{-1}). In our setup the detector signal is strictly proportional to the current in the storage ring assuming a stable electron orbit. The stability has recently been improved by the installation of a global feedback system [13]. This, plus the wedged beamline window and thick chamber windows, make it possible to work at 1 cm^{-1} resolution without suffering interference problems and with fluctuations less than 0.1% in 10 minutes.

The Cu sample was first mechanically polished, using a cerium oxide polishing compound for the last stage, and then electropolished in a 70% phosphoric acid/ 30 % distilled water solution with a constant current density of 0.07 A cm^{-2} applied for ~ 1 minute. Subsequent electron channeling patterns, acquired from a secondary electron microscope (JSM 6400) operated at 25 keV and 6 deg. grazing incidence, revealed high quality Kikuchi bands indicating good crystal quality in the surface region. Sputtering was done at $1x10^{-4}$ torr of Ne^{+}, at 500 eV and 300 K for 20 minutes, with the sample rotated to grazing incidence (both directions). The crystal was then annealed for 1 minute at 850 K. Auger spectra showed no sulfur, carbon or oxygen peaks, with an upper limit on the detection of < 1% of the copper (105 eV) peak. The measurements were all made at a base pressure of < 1 x 10^{-10} torr.

The infrared experiments were performed as follows. Two spectra of the clean sample were collected and ratioed to determine the stability and reproducibility of the synchrotron beam. If the reproducibility was better than 0.05% over the region of interest in 200 seconds collection time, then the sample would be dosed by backfilling the chamber with CO or NO gas. The final spectrum was collected within 12 minutes of the first clean sample spectrum. The results shown in the next section are the division of the co-added dosed spectra by the co-added clean copper spectra. Absolute changes in reflectivity were determined by normalizing to the exponentially decaying beam current. This procedure was found to be reliable within ±0.2% for the Cu-doped Ge detector.

3. RESULTS

Fig. 1 shows a comparison between the reflectivity spectra for a $(\sqrt{3}\times\sqrt{3})R30°$ (θ=0.33

monolayers) CO/Cu(111) and a θ=0.45 monolayer coverage of NO/Cu(111) [14]. The striking similarities between the two spectra are the background slope and the appearance of an anti-absorption feature at 285 and 328cm^{-1} respectively. One difference in the data is the appearance of a strong absorption peak for the carbon-metal stretch for CO, with no equivalent absorption for the NO. The CO data were taken at a resolution of 1 cm^{-1}, but for the NO data a resolution of 6 cm^{-1} was found to be adequate. This resolution difference is responsible for the lower noise in the NO data. Both sets of data were taken at 88K, the CO dose being 1.5 L and the NO dose 1.1 L. The NO coverage was chosen to maximize the intensity of the 328 cm^{-1} mode.

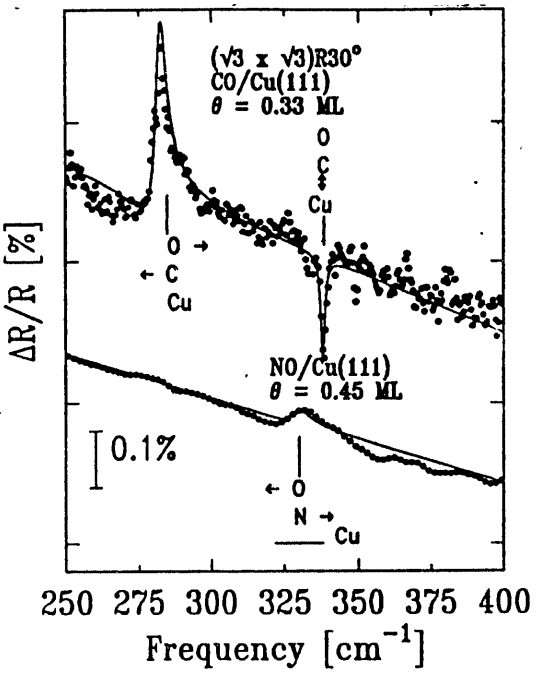

Fig. 1. Measured change in reflectivity observed for (√3×√3)*R*30° CO/Cu(111) (0.33 ML coverage) and 0.45 ML coverage of NO/Cu(111). The dots represent the data, the solid lines are fits as described in the text.

In Fig. 2, we show three spectra corresponding to 1.1 L dose of NO/Cu(111) and two isotopic substitutions, $^{15}N^{16}O$ and $^{14}N^{18}O$. Note that the frequency of the anti-absorption feature mentioned in the last paragraph shifts with the nitrogen mass, but not with the oxygen mass indicating that it is a hindered rotational mode [2]. It is assumed that the NO is bonded with the nitrogen atom closest to the metal. The spectrum for the $^{14}N^{18}O$ isotope, which is less pure, appears to show a broader feature, and is noisier due to less averaging.

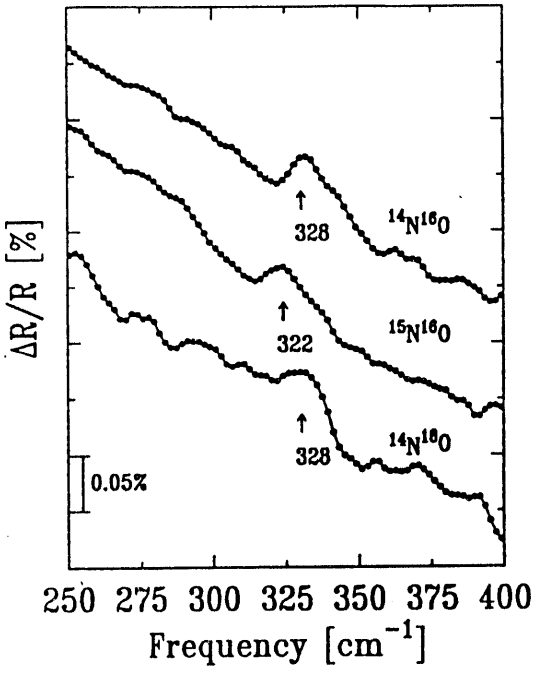

Fig. 2. Measured change in reflectivity observed for a θ=0.45 coverage of NO/Cu(111) for various isotopes of NO.

In Fig. 3, we show the measured change in reflectivity induced by CO and NO over the range 2500 cm^{-1} to 30 cm^{-1} with the same optical arrangement as in the previous data, but a different detector. Both spectra show a single symmetric high frequency absorption suggesting that the copper crystal has a low concentration of defect sites. The feature seen on both spectra at about 1200 cm^{-1}, can be moved by changing the mirror velocity for the rapid scan interferometer, confirming that it is an artifact. It

corresponds to radio frequency electron beam vibrations at ~1180 Hz. The two spectra appear to have a similar overall shape and are seen to fit well with the expression (next section) proposed by Persson[5]. The renormalized data have an absolute error of about ±0.2%. It is a coincidence that the absorption for both of these systems is the same within this error.

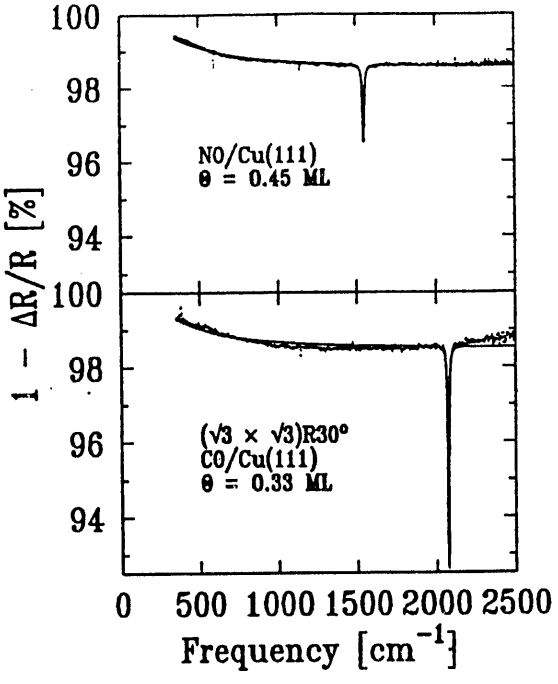

Fig. 3. Absolute change in reflectivity for CO/Cu(111) and NO/Cu(111) normalized to beam current (see text). The dots represent the data, the solid lines are fits as discussed in the text.

4. DISCUSSION

The data for both the CO/Cu(111) and NO/Cu(111) display qualitatively the same features. Both systems show 1. A high frequency Lorentzian absorption associated with a dipole allowed intramolecular stretch, 2. A low frequency, anti-absorption feature assigned to the hindered rotation mode [2], and 3. A broad-band background absorption. However, the low frequency CO/Cu(111) data has an additional absorption feature associated with the carbon-metal stretch which has no equivalent in the NO/Cu(111) data.

For CO/Cu(111) the data presented here show stronger, sharper features for both the carbon-metal mode and the hindered rotation mode, than we have published before [3]. In the previous measurements [3] a mechanically polished surface was used in contrast to the electro-chemically polished surface used here. Thus the hindered rotation mode involving motion parallel to the surface is also susceptible to inhomogeneous broadening. In fact we find that both this and the carbon-metal mode are much more sensitive to the morphology of the surface than the internal stretch mode.

In Fig. 1, the solid lines are fits to the data. In each case the background was fitted by a least squares method to a straight line over the limited frequency range 430-200 cm^{-1}. Then the lower frequency hindered rotation mode was fitted to the formula for a Fano line shape, developed by Langreth [4] for the line-shape of a vibrational mode arising from an electron-hole-pair decay process, thus:

$$L(\omega) = 4\left[\frac{\omega_r}{\omega}\right]\left[\frac{\mu_1^2}{\gamma}\right]\frac{(1-\omega\tau x^2)}{(1+x^2)} \qquad (1)$$

where $x=(\omega^2-\omega_r^2)/\gamma\omega$. ω_r is the fully renormalized Born-Oppenheimer vibration frequency, ω the probing radiation frequency, μ_1 the real part of the net dynamic dipole moment, γ the width of the electronic damping and $\omega\tau$ the phase delay. τ is the asymmetry parameter with $\tau=0$ giving a Lorentzian lineshape. This Fano [15] lineshape arises from an interference between discrete and continuum excitations. In practice, γ is proportional to the width of the peak, and μ_1 to its amplitude. Finally the carbon-metal stretch was fitted to a Lorentzian. The modes are sufficiently well separated to allow convergence with very few iterations.

From the fits to Fig. 1, the FWHM of the carbon-metal mode, with its Lorentzian lineshape, is straightforward to determine and has a surprisingly narrow line-width of 1.7cm^{-1}. The determination for of the linewidth for the asymmetric lineshapes of the frustrated rotations is more difficult because of the asymmetry parameter; i.e. the fits are not uniquely determined. Good fits were obtained with widths of of 4.6 cm^{-1} and 6.5 cm^{-1} for CO and NO, respectively, and an asymmetry (τ) of -.001 for both. The quality of the fits was seriously lower for linewidths greater than 6 and 8 cm^{-1} for CO and NO respectively.

The hindered rotational mode of NO is broader and an order of magnitude weaker than that of CO. This may be due to differences in the adsorption site. Though it is established that CO sits at atop sites [16], the site for the NO adsorption is not exactly known. The N-O stretch at 1551 cm^{-1}, represents a 450 cm^{-1} shift from the gas phase value, from which So et al. [6] suggest that bridge sites are occupied. More recently, calculations suggest that the bridge site geometry is highly tilted and that the shift is consistent with three-fold sites [7]. In any case, recent NEXAFS work for NO on Ni(111) [17] has demonstrated that interpretations of site geometry from frequency shifts must be treated with caution. With bridge site or tilted configurations, the degeneracy of the hindered rotation modes is lifted. Thus the weakness of the NO mode could be attributed to coupling to only one of these modes. However calculations for CO/Ni suggest large shifts of ± 200 cm^{-1} in the frequency of the two hindered rotational modes on switching from atop to bridge sites [18]. Although this is a completely different system, it seems unlikely that the present peak at 328 cm^{-1} could represent a mode shifted by so much.

There is no apparent strong nitrogen-metal mode in the low frequency NO/Cu data but the fit without a Lorentzian lineshape added in suggests that there could be a broad (FWHM ~25 cm^{-1}) feature in the data. Since a LEED pattern could not be seen for this system it is likely that the N-Cu stretch is significantly broadened by inhomogeneous effects. Also the coordination of the molecule may be playing a role. For example, the observed strength of the H-substrate stretch is a function of the coordination of substrate atoms for the adsorption site. It is strongest for the atop H/Si system [19], less strong for the two-fold coordinated bridge site occupation of H/W(100)[1], and even weaker for H/Pt [20] which has three fold hollow sites filled.

Finally, we discuss the change in the background for these two systems. This absorption looks qualitatively the same for both systems and can be compared to O/Cu(100), and CO/Cu(100) [21]. The absorption bands for adsorbate systems on copper all have basically the same shape which approach an asymptotic limit of ~1% at 2300 cm^{-1} for a coverage of ~0.5 ML.

Persson and Volokitin [22] have proposed a theory based on coupled equations of motion for adsorbates and conduction electrons for a jellium substrate. The adsorbate motion parallel to the surface couples to the induced current parallel to and beneath the surface. There are two major consequences of this theory. The first is a broadband background absorption, due to the non-specular scattering of the conduction electrons when the adsorbates are present. The second is that all adsorbate modes parallel to the surface, the dipole forbidden modes, are observed as anti-absorption peaks. This is because there is no relative motion between the vibrating adsorbate and the collective motion of the electron gas.

In Fig. 3, the broadband spectra for CO and NO/Cu(111) with fits (solid lines) are presented. The fits are based on a Lorentzian and the following formula which has recently been extended to include non-local optics [5]:

$$R = 1 - a\frac{\omega^2}{\omega^2 + \frac{6}{5}b^2} \qquad (2)$$

where a is the high frequency asymptotic limit, ω is the frequency of the incident light, and

$b=v_F/\delta$ with v_F equal to the Fermi velocity of the conduction electrons, and δ the skin depth of the substrate.

The expanded form of Eq. (2) shows that a is proportional to the relaxation rate of the damping of the hindered translation which is due to the excitation of electron-hole pairs [5]:

$$R = 1 - \frac{4Mn_a}{mnc}\frac{1}{\tau}\frac{1}{\cos\theta} \times \frac{[\Omega^2-\omega^2]}{[\Omega^2-\omega^2]^2+[\omega/\tau]^2}\frac{\omega^2}{\omega^2+\frac{6}{5}b^2} \qquad (3)$$

where the assumptions are that the light frequency $\omega \gg 1/\tau_B$ with τ_B the bulk relaxation time, and $\omega/\omega_p \gg v_F/c$ where ω_p is the plasma frequency. In Eq. 3 τ is the relaxation time, n_a is the adsorbate density, θ is the angle of incidence, and Ω is the frequency of the hindered translation. The fits shown in Fig. 3 were based on the high frequency limit since the hindered translation [23,24] is well below 100 cm^{-1}. The a parameters obtained from the fits correspond to relaxation times of 0.92 psecs for CO/Cu(111) and 1.4 psecs for NO/Cu(111). The b values used were 375 and 404 cm^{-1} respectively. These values are close to the prediction of the jellium model, $b=\omega_p(v_F/c) \sim 444$ cm^{-1}. This shows satisfactory overall agreement considering that copper is not jellium, and that we are not in the local-optics limit. Finally, the observance of the anti-absorption peak is also predicted by Eq. 3, as the second term on the right hand side goes to zero when the vibration of the hindered translation is the same as the frequency of the incident electric field. This behavior is expected to occur for all normal modes parallel to the surface on "Drude-like" substrates.

5. CONCLUSIONS

Hindered rotational modes have been observed in the far infrared for two adsorbate/metal substrate systems: CO and NO on Cu(111). These modes have asymmetric lineshapes, which, when analyzed, can provide some lower limit on the vibrational lifetimes and some insight on how the lineshape is affected by bonding. This difference maybe due to the fact that NO is more ionically bonded than CO and/or that its bonding site is of higher coordination than CO. The scattering theory appears to account well for the broadband absorptions accompanying the presence of these asymmetric lineshapes. This theory can be further tested by performing similar measurements on other systems. Also, measurements toward still lower infrared frequencies will make it possible to detect directly the hindered translation modes and further test the scattering theory.

ACKNOWLEDGEMENTS

Technical support at the beamline was provided by Dennis Carlson. The special crystal mounting was made by Ed Chaban. We are grateful for discussions with our colleagues, especially Bo Persson and Larry Carr. We also thank Carol Smyth and Chris Echols for their assistance during their stays with us at the U4IR beamline and to Kathy Warburton, Bob Sabatini and Michelle Taube for the help with crystal preparation and characterization. This work was supported by the United States Department of Energy under contract DE-AC02-76CH00016 and by the NSF International Collaborative Award INT-9016771.

REFERENCES

1. J.E. Reutt, Y.J. Chabal and S.B. Christman, Phys. Rev. B38 3112 (1988).

2. C. J. Hirschmugl, G. P. Williams, F. M. Hoffmann and Y. J. Chabal, Physical Review Letters 65 408 (1990).

3. C. J. Hirschmugl, G. P. Williams, F. M. Hoffmann and Y. J. Chabal, J. Electron Spectrosc. Relat. Phenom. 54/55 109, (1990).

4. D.C. Langreth, Phys. Rev. Lett. 54 126

(1985).

5. B.N.J Persson, Chem. Phys. Letts. 197 7 (1992).

6. S.K. So, R. Franchy and W. Ho, J. Chem. Phys 95 1385 (1991)

7. M. Fernandez-Garcia,, J.C. Conesa, F. Illas, Surf. Sci. 280 441 (1993)

8. T. Munakata, K. Mase, I. Kinoshita, Surf. Sci. 286 73 (1993).

9. Gwyn P. Williams, Int. J. Infrared Millimeter Waves 5 529 (1984).

10. G. P. Williams, Nuc. Instrum and Meth. A291 8 (1990).

11. Gwyn P. Williams, Rev. Sci. Instrum. 63 1535, (1992).

12. C.J. Hirschmugl, Nucl. Inst. Methods in Phys. Res. A319 245 (1992).

13. L.H. Yu, R. Biscardi, J. Bittner, E. Bozoki, J. Galayda, S. Krinsky, R. Nawrocky, O. Singh and G. Vignola, Proc. 1989 Particle Accelerator Conf., Chicago, IL, USA, p. 1792 (1989).

14. After the 1.1L NO dosed sample was exposed to the electron beam from the LEED gun a $p(3\times3)$ pattern corresponding to a coverage of θ=0.45 monolayers was observed with no apparent desorption. Further investigation of this is continuing.

15. U. Fano, Phys. Rev. 124 1866 (1961).

16. R. Raval, S.F. Parker, M.E. Pemble, P. Hollins, J. Pritchard, and M.A. Chesters, Surf. Sci. 203 353 (1988).

17. M.C. Asensio, D.P. Woodruff, A.W. Robinson, K.-M. Schindler, P. Gardner, D. Ricken, A.M. Bradshaw, J.C. Conesa, and A.R. Gonzalez-Elipe, Chem Phys Lett 192 259 (1992).

18. N.V. Richardson, and A.M. Bradshaw, Surf. Sci. 88 255 (1979)

19. Y.J. Chabal, Physica B 170 447 (1991).

20. J.E. Reutt, Y.J. Chabal, S.B. Christman, J. Vac. Sci and Tech. A6 816 (1988).

21. K. Lin, R. Tobin, C.J. Hirschmugl, G.P. Williams, P.Dumas, Phys. Rev. B, to be published.

22. B.N.J Persson, A. Volokitin, Chem. Phys. Lett. 185 292 (1991).

23. W. Akemann and A. Otto, J. Raman Spectrosc. 22 797 (1991).

24. J. Ellis and J. P. Toennies, private communication, November 1992.

DATE
FILMED
6/9/94
END